AIMETA '03
XVI Congresso AIMETA di Meccanica Teorica e Applicata
16th AIMETA Congress of Theoretical and Applied Mechanics

MODELING OF THE PULLOUT TEST THROUGH THE CELL METHOD

E. FERRETTI, A. DI LEO

[1] *Dipartimento di Ingegneria delle Strutture, dei Trasporti, delle Acque, del Rilevamento, del Territorio (DISTART), Università di Bologna – Alma Mater Studiorum, Bologna*

SOMMARIO
Il codice con automatico remeshing al Metodo delle Celle (CM) per l'analisi della propagazione della frattura viene usato per modellare la prova di pullout. Le interpretazioni degli studi sperimentali ed analitici sul pullout variano enormemente e nessuna delle spiegazioni avanzate a tutt'oggi offre una descrizione completa della crisi progressiva del calcestruzzo. L'analisi dello stato limite è stata qui condotta per diversi rapporti tra cerchio di contrasto e profondità di infissione. Si è inoltre ottenuto il percorso completo di propagazione per la geometria del Lok-test. Viene anche fornito lo stato tenso-deformativo evolutivo per il Lok-test. L'identificazione delle direzioni principali di tensione completa l'analisi tensionale.

ABSTRACT
The Cell Method (CM) code with automatic remeshing for crack propagation analysis is here used for modeling the pullout test. The interpretations of experimental and analytical studies on the pullout test vary widely, and none of the existing explanations offer a complete description of the progressive failure of the concrete medium. Here, failure analysis has been performed for several ratios between the counter-pressure diameter and the stem length. Moreover, the complete crack path has been obtained for the geometry of the Lok-test. The evolving state of stress-strain for the Lok-test is also provided. The identification of the directions of principal stress completes the stress analysis.

1. THE PULLOUT TEST PROCEDURE

The pullout test is a nondestructive test procedure which has been suggested by many as an in-place testing procedure alternative to testing field-cast cylinders in the laboratory. The test procedure involves pulling out an anchor plate embedded in concrete with the aid of a tensile jack. During application, a test bolt, consisting of a stem and a circular steel disc, is mounted inside the form (Fig. 1(a)). After curing the concrete, the form is stripped, and the stem is unscrewed. At the time of testing, a rod having a slightly smaller diameter than the stem is screwed into the disc and a cylindrical counter-pressure is mounted (Fig. 1(b)). The rod is loaded by a pullout force until failure, where a small piece of concrete can be punched out if sufficient displacement of the rod is applied.

Requirements for the testing configuration are given in ASTM C 900. The embedment depths (that is, the stem length) and head diameter must be equal, but there is no requirement on the magnitude of these dimensions. Commercial inserts have embedment depths about 25 to 30 mm. The inner diameter of the reaction ring can be any size between 2.0 and 2.4 times the insert-head diameter. This means that the apex angle of the conic frustum defined by the insert-head diameter and the inside diameter of the reaction ring ($2a$ in Fig. 1) can vary between 54 and 70 deg. The test apparatus and procedure for the Danish version of the pullout test, the Lok-Test, are illustrated in Fig. 1 [1]. This geometry has been proposed by Kierkegaard-Hansen [2].

Extensive field investigations on pullout test have been conducted in Europe, Canada, and the United States. A detailed summary on relevant works can be found in Yener and Chen [3]. All laboratory tests indicate that the failure surface is trumpet shaped (Fig. 2). The large diameter of the fragment is determined by the inner diameter of the reaction ring, and the small diameter is determined by the insert-head diameter.

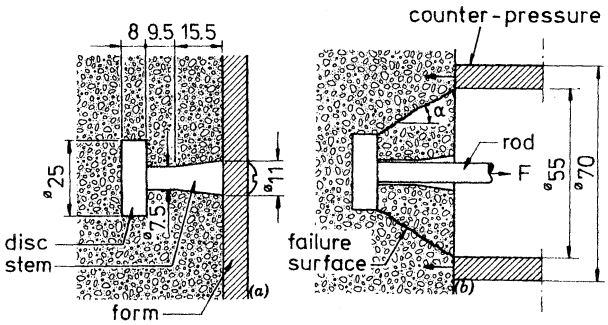

Fig. 1: Application and configuration of Lok-Test (all dimensions are in millimeters)

Fig. 2: Shape of the extracted concrete portion

It was found that the pullout force can be linearly related to the compressive strength measured from standard cylinders or cubes [4]. This relationship is not significantly affected by variations in water-cement ratio, type, shape and size of aggregates up to 40 mm maximum aggregate size, type of cement, curing conditions (water cured, cured in air and maltreated), curing time, admixtures, flyash, and air content. Only the use of lightweight aggregates produces a significantly differ correlation [5]. Most of the existing hypotheses seem then to describe the behavior of concrete in pullout tests through a uniaxial phenomenon. In spite of that, there has been a considerable amount of controversy regarding the property of concrete that is actually measured in pullout tests [4]. It is not clear whether tension, compression, shear, or punching shear strength of concrete is measured, and what constitutes the physical mechanism of failure. Past tests, confirmed by theoretical considerations based on plastic failure of concrete, have shown that the pullout force essentially depends upon compressive strength only for angles $a = 30° \div 35°$ [6]. For angles greater than 45° it depends instead, by a constant proportionality, mostly upon tensile strength.

2. GENERAL REMARKS ON THE REMESHING CM CODE

The theoretical basics of the Cell Method (CM) have been developed by Tonti [7]. The essence of the CM is to provide a direct finite formulation of field equations, without requiring a differential formulation. The CM uses two meshes, the one the dual of the other (Fig. 3). In crack propagation problems, the geometry of the mesh must be modified as the

crack propagates. The ability of the CM code with remeshing to take a general change in the mesh topology easily into account has been shown in [8]. This ability is all the more relevant since changes in mesh topology are rarely supported by classical finite element method (FEM) numerical codes.

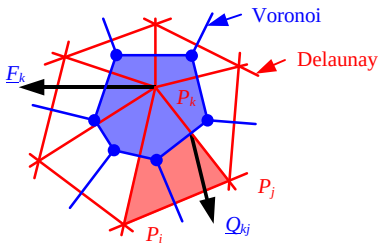

Fig. 3: Mesh of Delaunay/Voronoi

In the CM code with remeshing, the crack has been modeled as a displacement discontinuity. For modeling the crack propagation through the mesh, as required by this strategy, the nodal relaxation technique has been adopted. This technique can be achieved using inter-element propagation or intra-element propagation (Fig. 4). Inter-element propagation is mesh dependent, since the crack propagates along the mesh side nearest to the computed propagation direction. On the contrary, intra-element propagation is mesh independent, since the crack propagates along the computed propagation direction. This takes more computational time for regenerating the mesh, but leads to more accurate results. The code here employed uses the nodal relaxation with intra-element propagation technique.

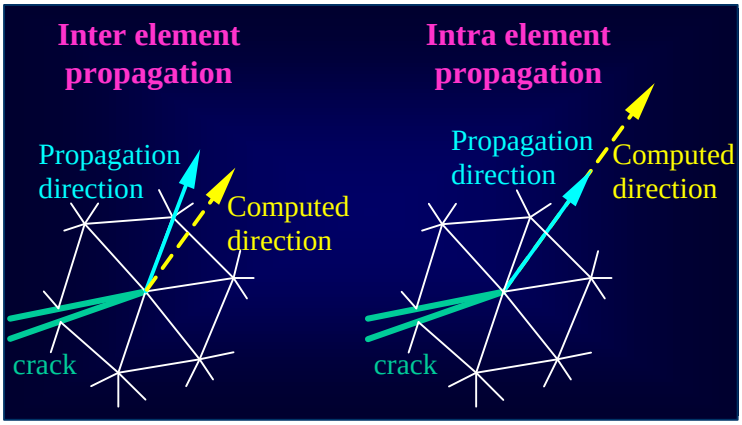

Fig. 4: Inter and intra element propagation for the nodal relaxation technique

Finally, a special hexagonal element has been inserted at the crack tip (Fig. 5), for regularizing the shape of the mesh surrounding the tip. Since the CM associates geometrical objects of the dual mesh to source variables, this regularization allows description of the stress field in a finite neighborhood of the tip [8]. In the remainder of the domain, the mesh generator is allowed to generate the mesh automatically. Further details on the remeshing CM code are collected in [8].

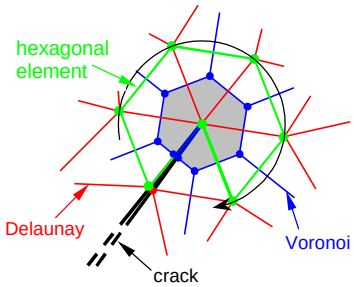

Fig. 5: Special element for stress analysis

3. CONSTITUTIVE ASSUMPTIONS

The concrete constitutive law adopted in this study is monotonically non-decreasing (Fig. 6), in accordance with the identification procedure for concrete in mono-axial load provided by Ferretti [9]. It was shown [9, 10] how the monotone law identified by Ferretti [9] turns out to be size and failure mechanism insensitive for mono-axial compressive load. This result made it possible to formulate a new concrete law in mono-axial compressive loading, the

effective law, which can be considered to be more representative of the material physical properties than the softening laws are.

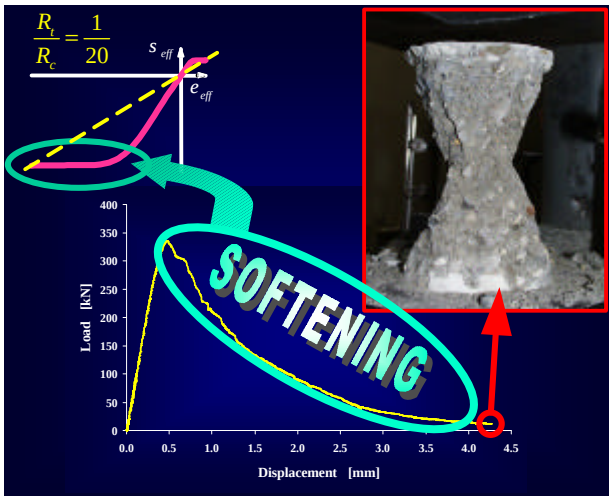

Fig. 6: Identified effective law for concrete

4. NUMERICAL RESULTS

Numerical results concerning the pullout test modeling through the remeshing CM code will be presented here.

One analysis on the extinction zone of the load transferred by the steel insert has been performed, in order to identify the minimum finite geometry correctly reproducing the stress-strain field around the steel insert. For simplicity, the minimum finite geometry has been assumed to be square shaped. This geometry has then been used as modeling domain in the CM remeshing code.

4.1. Identification of the unknown boundary conditions

The pullout test is a typical example of crack propagation in Mixed Mode loading, since the load is applied obliquely both to the crack propagation direction and to the crack opening direction. For such a type of load, the combination of loading and boundary conditions forces the edges of the crack to close at some point. At those points, Mode II loading prevails. At the remaining points, the two edges of the crack separate and Mode I loading prevails. Points separating the zones in which Mode I loading prevails from those in which Mode II loading prevails are a function of the load step and crack length. They thus represent an unknown of the Mixed-Mode problem and must be identified before the numerical stress analysis takes place.

Not only the crack edges are subjected to Mixed-Mode loading in the pullout test. There are indeed other surfaces which can separate or slide over each other, developing constraint reactions. They are the surfaces separating the steel insert from the concrete specimen. In this second case, the surfaces cannot evolve, but the point separating the Mode I loading zone from the Mode II loading zone is still an unknown of the Mixed-Mode loading problem.

As has been shown in [8], the CM remeshing code is automatically able to estimate which part of the boundary is subjected to Mode I loading, and which part is subjected to Mode II loading. The result of the boundary condition identification on the surface separating the insert disk from the concrete specimen is shown in Figs. 7 for the geometry of the Lok-Test.

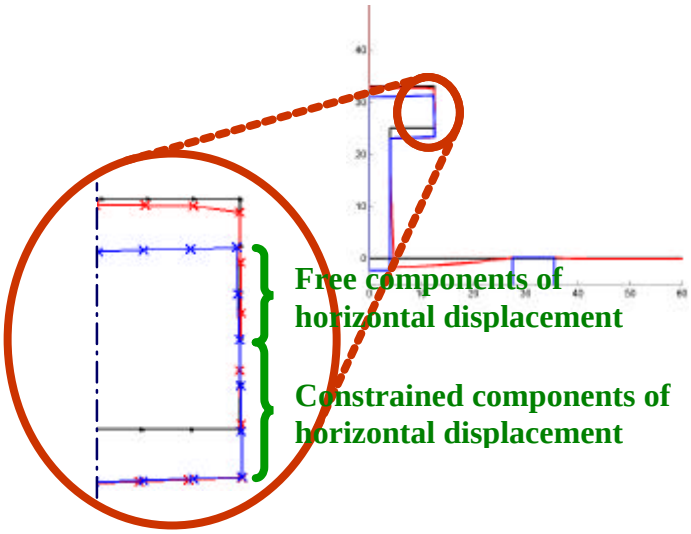

Fig. 7: Deformed configuration and detail of the identified boundary conditions on the disk thickness

4.2. Analysis of the stress field

The simulation has been performed in displacement-control, by imposing the relative displacement between the rod lower edge and the counterpressure ring upper edge. The counterpressure ring has been assumed to be perfectly rigid. It has been considered as an external constraint, and it does not belong to the modeled domain. The zero value of absolute vertical displacements on the external boundary has been fixed on the lower right corner of the extinction zone (assumption of zero displacement at infinity). For this choice of absolute displacement, it was possible to estimate the punching effect on the concrete-counterpressure ring interface.

The bond between the pullout disk and the concrete above the disk has been assumed to be monolateral, with the steel nodes free to move downward with regard to the concrete nodes, from the beginning of the test forth.

A number of graphical tools were developed together with the CM remeshing code [9], in order to draw the stress-strain field in the modeled domain. The graphical tool for the principal directions drawing provides each Delaunay element with a segment centered on the element circumcenter, whose direction is that of the principal direction, and whose length is scaled by the principal stress (Fig. 8). Principal directions and principal values are computed in the element circumcenter.

The CM analysis of the stress field between the steel insert and the counterpressure ring (Fig. 8) exhibits very large a stress transferring zone of compressive forces.

As will be discussed in the following, the stress transferring zone grows thin as the crack propagates from the disk toward the counterpressure ring. Approaching the ultimate load, a narrow compressed band of stress transferring can be identified, as in the analysis of Ottosen [1]. The large portion of specimen interested by the stress transferring mechanism before cracking is also given by the graphic tool for the stress discrete drawing in the axial direction (Fig. 9). Fig. 9 also shows the pouncing effect on the stress field at the disk-specimen and counterpressure ring-specimen interfaces.

The stress field analysis is completed by the tool for computing the crack propagation direction proposed in [8]. The analysis in the Mohr-Coulomb plane and the crack geometry updating before remeshing activation are the same as in [8]. The difference between the present numerical simulation and the one presented in [8] concerns the failure criterion, since, this second time, the Leon criterion was used. The two directions of first propagation for the

Lok-test geometry are shown in Fig. 10. They are given by the directions of the lines that join the Mohr's pole to the two tangent points. When the limit condition is reached, both the directions activate, and two cracks then enucleate. The direction with the minimum slope (in magnitude) with regard to the s axis was denoted as first direction of propagation, and the direction with the maximum slope (in magnitude) with regard to the s axis was denoted as second direction of propagation (Fig. 10). Since experimental results show that the crack along the first direction of propagation stops soon after its initiation [11], only the second direction of propagation has been considered in the numerical simulation. The crack paths presented in the following are then relative to the second direction of propagation.

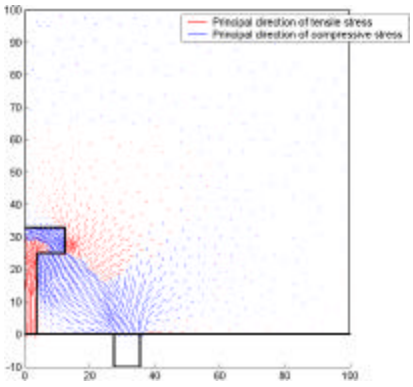

Fig. 8: Numerical principal directions and principal stresses for the geometry of the Lok-test

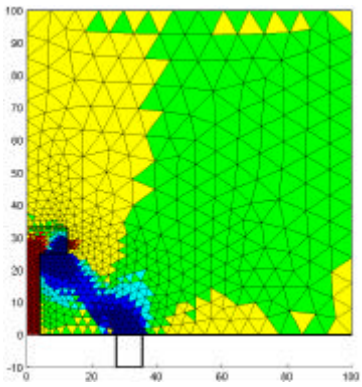

Fig. 9: Discrete stress analysis for the geometry of the Lok-test

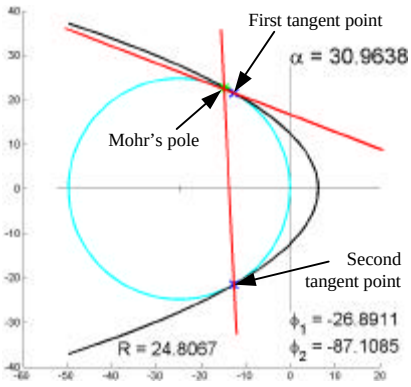

Fig. 10: Limit condition and directions of first propagation for the geometry of the Lok-Test

4.3. Analysis of the mechanism of crack initiation

Experimental results show that the crack initiation mechanism in the pullout test depends on the geometry of the pullout apparatus [12]. In particular, the ratio between the internal diameter of the counterpressure ring and the rod depth is decisive in establishing the type of failure process. That is, the failure mechanism depends on the angle a, defined as in Fig. 1. Nevertheless, experimental results are not exhaustive in describing the dependence of the initiation mechanism from a. This leads to the impossibility of identifying a unified model, able to correctly describe the failure mechanism for varying values of a. Such a type of model is of fundamental importance when a numerical analysis based on the equilibrium of the concrete to be extracted is attempted [13]. In this work, the CM remeshing code is proposed as an analysis instrument for identifying the correlation between initiation mechanism and a. This is possible since the CM remeshing code operates on both the steel and concrete domains, automatically computing the boundary conditions on the steel-concrete interface. The definition of a steel-concrete behavior model is not needed and the simplified numerical analysis of equilibrium on the concrete to be extracted is not required. No a-priori assumptions have then been done on the steel-concrete interaction. This last has been identified a-posteriori, as an output of the numerical simulation.

The angle a (Fig. 1) has been chosen as the geometrical parameter of the steel-concrete interaction. In the following, all values of α will be provided in degrees.

The analysis of the initiation mechanism has been performed in the Mohr-Coulomb plane, such as in [8]. The failure criterion adopted is the Leon criterion. For this criterion, the limit surface in the Mohr-Coulomb plane is parabolic (Fig. 10).

The initiation point has been fixed on the right-bottom corner of the disk (Fig. 11), in agreement with experimental [11] and previous numerical results [1, 14, 15, 12, 4]. On this

point, the special element for stress analysis has been inserted (Fig. 11). The special element used here is a refinement of the special hexagonal element used in [8] (Fig. 5), which was studied to be inserted at the crack tip of pre-cracked specimens.

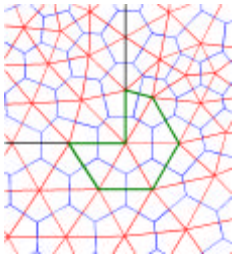

Fig. 11: Special element for stress analysis on the domain contour

In pullout test, the direction of first propagation is an unknown of the problem, since it is one of the quantities affected by the dependence from a. Consequently, pre-cracking was not possible. The special element for stress analysis was then inserted on the known point of initiation, which is a point of the steel-concrete interface. To prevent the special element from intersecting the steel-concrete interface, the geometry of the special element for the first propagation step has been modified as shown in Fig. 11. For further propagation steps, the same hexagonal element as the one used in [8] has been inserted at the crack tip.

The load of crack initiation has been computed from the step-wise identification of the (relative) displacement of crack initiation (simulation in displacement-control). Once the load of crack initiation has been identified, the intersection points between the corresponding Mohr's circle and the limit surface give the mechanism of failure initiation.

In Fig. 10, the two intersection points lie in the negative semi-plane of the normal stress. Both the corresponding values of shear and normal stresses are not negligible. One can then conclude that the value of the angle a equal to 30.9638° corresponds to a mechanism of failure initiation for shear-compression. From the analysis in the Mohr plane, it was found that the failure mechanism for $a < 63.4349°$, $a = 63.4349°$, $63.4349° < a < 71.5651°$, and $a \geq 71.5651°$ is, respectively, of shear-compression, pure shear, shear-traction, and pure traction.

4.4. Crack propagation analysis

A step-wise analysis of crack propagation has been performed for the pullout geometry of the Lok-Test.

According to the discrete crack approach, a modification of the mesh is required at each step of the crack propagation process. The tool here adopted for crack geometry updating and remeshing is described in [8].

The numerical crack path and the stress analysis predicted by the numerical model are shown in Fig. 12 for four failure stages. In accordance with the experimental results (Fig. 2), the numerical direction of propagation changes at every stage. In particular, after a sub-vertical propagation the propagation direction changes abruptly and the crack propagates towards the counterpressure ring. The intra-element propagation technique and reduction of the mesh size near the crack tip allow the crack path to be accurately predicted. From the stress and principal directions analysis in Fig. 12 one can conclude that the static scheme of the resistant structure changes at each propagation step. In particular, at first the resistant structure is subjected to compressive stresses in the disk-counterpressure ring direction. For this stage, the principal stresses are nonuniform and the principal directions are not parallel to each other, as in the linear-elastic finite element analysis of Stone and Carino [14]. As the crack propagates, bending actions superimpose to the compressive stresses. As a consequence, the transferring zone of compressive stresses becomes thinner and thinner, and the non-uniform stress behavior is enhanced. The comparison of a neutral axis in the concrete to be extracted arises simultaneously to the radical changing in the crack propagation direction.

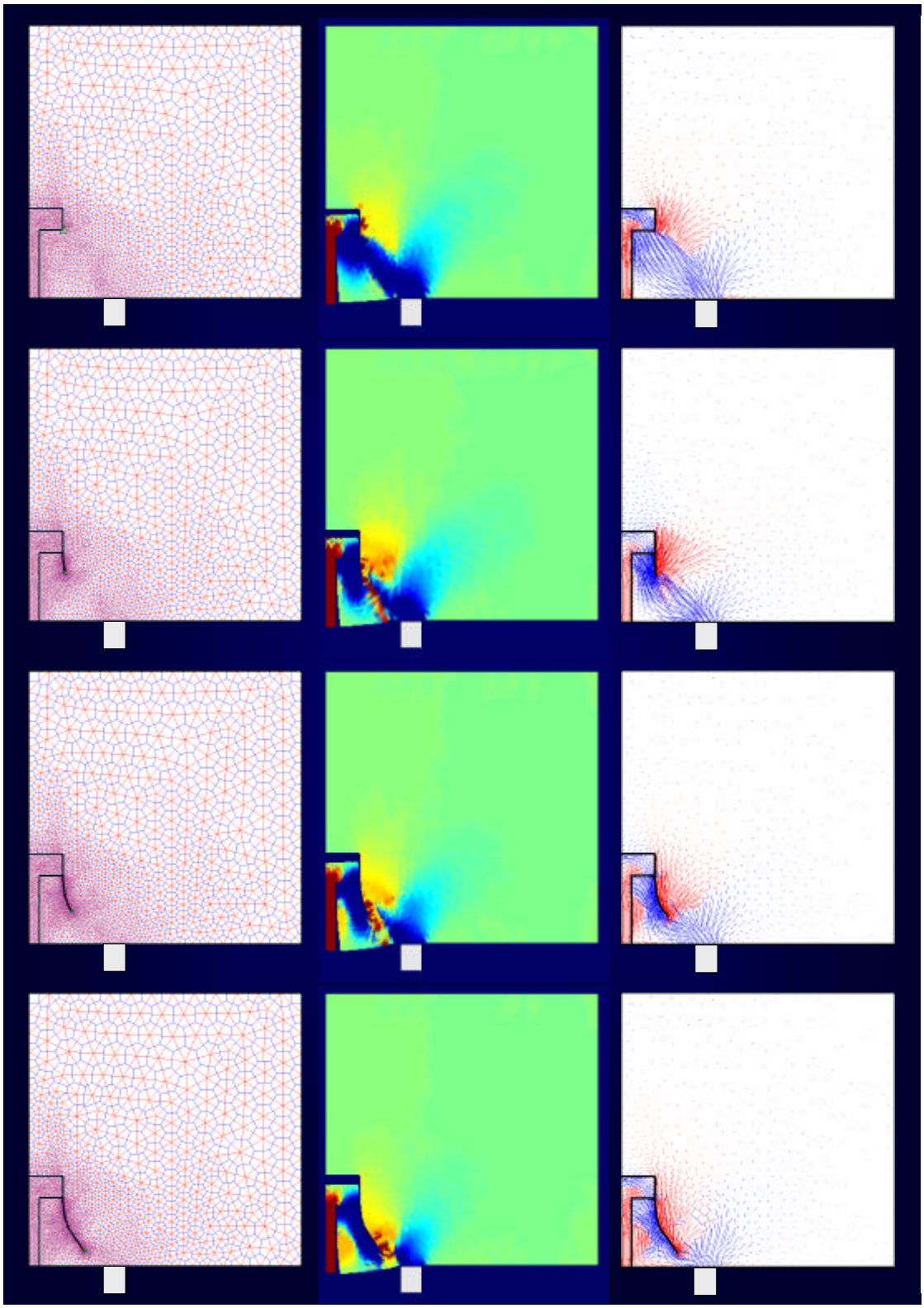

Fig. 12: Mesh, stress and strain analysis for four failure stages (geometry of Lok-Test)

In the stress analysis for the third stage of Fig. 12, changing of the crack propagation direction and comparison of a tension zone near the stem are well recognizable. During the latter stages of crack propagation the bending actions become dominant. It can than be concluded that crack propagation also involves progressive bending of the compressed

concrete within the concrete to be extracted. This result agrees with the plastic-fracture finite element analysis of Yener [4].

The third stage of Fig. 12 also shows a modification of the stress field in front of the crack tip. In particular, a tensile state of stress with principal direction perpendicular to the crack last edge is well recognizable. Since the crack direction will remain unchanged from this moment forth, it is reasonable to conclude that the tensile state of stress contributes to crack propagation in this last phase of the pullout test. Also opening of the crack edges behind the crack tip confirms this assumption (Fig. 12, deformed configuration of third stage).

5. CONCLUSIONS

A CM code has been used here both for crack initiation and crack propagation analysis in the pullout test modeling. Several ratios between the internal diameter of the counterpressure ring and the rod length have been taken into account for the crack initiation analysis. The crack propagation analysis has been performed for the geometry of the Lok-Test.

The adopted CM code combines nodal relaxation, intra-element propagation and remeshing. It also permits the mesh dimensions to be refined at specific locations, so as to improve the accuracy of the solution. The mesh generator ability to operate on multiple domains has been used to provide the evolving stress field both in the steel insert and concrete specimen. Finally, the code automatically estimates which part of the boundary is subjected to Mode I loading, and which part is subjected to Mode II loading. Consequently, no a-priori assumptions are needed on the steel-concrete interaction. The computation is then performed on the whole domain, without having to reduce the analysis on the equilibrium condition of the extracted concrete.

The simulation is displacement-controlled. The agreement between CM results and results of previous FEM analysis further states that the CM can give good predictions for fracture mechanics problems. Also the experimental results are well reproduced.

The step-wise analysis of the state of stress allows us to describe the progressive failure of the concrete medium. It was found that the crack initiation mechanism depends upon the ratio between the internal diameter of the counterpressure ring and the rod length. A changing in the crack initiation mechanism from shear-compression to shear-tension was found to occur for the angle a equal to about 63°. Moreover, the crack propagation mechanism changes as the crack propagates. At first, the concrete between the steel disk and the conterpressure ring is compressed in the disk-ring direction. Subsequently, bending actions develop in the concrete fragment to be extracted. They become more and more relevant with the evolving of the failure process and a neutral axis arises in the concrete fragment. Compressive interactions between steel rod and concrete specimen and the punching effect at the disk-concrete interface cause the neutral axis to intersect the rod-concrete interface, never arriving at the disk-concrete interface. The direction of the neutral axis is more or less parallel to the crack direction. The comparison of the neutral axis seems to be correlated to the abrupt change of the crack propagation direction, also experimentally observed. From the moment in which the crack direction changes on, a tensile state of stress develops in front of the crack tip. It may then be reasonable to assume that tensile strength of the concrete has some kind of indirect influence on the pullout strength. It can be concluded that it may be not appropriate to describe the complex state of stress induced in pullout test by a uniaxial mode of failure. It can also be asserted that an alternative explanation needs to be found for the experimentally observed close correlation between compressive and pullout strength.

The analysis of the stress field provides a detailed description of the stress redistribution with the crack propagation. It seems then that the CM code is able to provide a substantial contribution to the comprehension of the physical mechanism of failure in pullout tests.

The analysis performed has been carried out by following only one of the two experimentally observed crack paths. Numerical results can improve if the second crack path is modeled as well. Further studies are currently being undertaken to activate the second propagation and study the mutual influence between the two cracks. Moreover, an extension of the code in such a way as to take into account the friction between the nodes lying on the crack edges is being studied at the present time. Finally, also combination of concrete crushing and concrete cracking is under study at the moment, so as to derive the complete load-displacement diagram in pullout tests.

REFERENCES

[1] Ottosen N. S.: Nonlinear Finite Element Analysis of Pull-Out Test, *Journal of the Structural Division*, vol. 107, No. ST4, pp. 591-603 (1981).

[2] Kierkegaard-Hansen P.: Lok-Strength, *Nordisk Betong (Journal of the Nordic Concrete Federation)*, No. 3, pp. 19-28 (1975).

[3] Yener M., Chen W. F.: On In-Place Strength of Concrete and Pullout tests, *Journal of Cement, Concrete, and Aggregates*, Vol. 6, No. 2, pp. 90-99 (1984).

[4] Yener M.: Overview and Progressive Finite Element Analysis of Pullout Tests, *ACI Structural Journal*, Vol. 91, No. 1, pp. 49-58 (1994).

[5] Petersen C. G.: Lok-Test and Capo-Test Development and Their Applications, *Proceedings, Institution of Civil Engineering*, Part I, 76, pp. 539-549 (1984).

[6] Bocca P.: The application of Pull-Out Test to High Strength Concrete Estimation, *Matériaux et Constructions*, Vol. 17, No. 99, pp. 211-216 (1984).

[7] Tonti E.: A Direct Discrete Formulation of Field Laws: the Cell Method, *CMES*, Vol. 2, No. 2, pp. 237-258 (2001).

[8] Ferretti E.: Crack Propagation Modeling by Remeshing Using the Cell Method (CM), *CMES*, Vol. 4, No. 1, pp. 51-72 (2003).

[9] Ferretti E.: Modellazione del Comportamento del Solido Cilindrico Compresso, Ph.D. Thesis, University of Lecce, Italy (2001).

[10] Ferretti E., Bastianini F.: Identification of the Local $s_{eff} - e_{eff}$ Law for Concrete under Uniaxial Monotone Compression, *Proc ABDM*, full text on CD-ROM (16 pp.) (2002).

[11] Krenchel H., Bickley J. A.: Pullout Testing of Concrete. Historical Background and Scientific Level Today, *Nordic Concrete Research*, Publ. No. 6, The Nordic Concrete Federation (1985).

[12] Bocca P., Carpinteri A., Valente S.: Evaluation of Concrete Fracture Energy Through a Pull-Out Testing Procedure, *Fracture of Concrete and Rock*, pp. 347-356 (1989).

[13] Jensen B. C., Bræstrup M. W.: Lok-Tests Determine the Compressive Strength of Concrete, *Nordisk Betong (Journal of the Nordic Concrete Federation)*, No. 2, pp. 9-11 (1976).

[14] Stone W. C., Carino N. J.: Comparison of Analytical with experimental Internal Strain Distribution for the Pullout Test, *ACI Journal*, Vol. 81, No. 1, pp. 3-12 (1984).

[15] Hellier A. K, Sansalone M, Carino N. J, Stone W. C., Ingraffea A. R.: Finite-element Analysis of the Pullout Test Using a Nonlinear Discrete Cracking Approach, *Journal of Cement, Concrete and Aggregates*, Vol. 9, No. 1, pp. 20-29 (1987).